GEARSolutions

Large Measuring Centers Ready for Large Tasks

ISSUE FOCUS

Gear Design & Inspection

COMPANY PROFILE:
CGI, Inc.

Your Resource for Machines, Services, and Tooling for the Gear Industry

Analysis of Tooth Interior Fatigue Fracture Using Boundary Conditions from an Efficient and Accurate LTCA

By Baydu Al and Paul Langlois

Utilizing MASTA's 3D Loaded Tooth Contact Analysis model, a modified methodology is proposed to predict crack initiation risk for tooth interior fatigue fracture.

THIS PAPER DEMONSTRATES A MODIFICATION TO the analysis of Tooth Interior Fatigue Fracture, as implemented in SMT's MASTA software, in which Loaded Tooth Contact Analysis (LTCA) results from a specialized 3D elastic contact model have been utilized to determine the load boundary conditions for analysis of Tooth Interior Fatigue Fracture (TIFF) to the method of MackAldener. In contrast to MackAldener's method, using finite element contact analysis, this method allows for quick analysis times for the calculation of the stress history leading to fast optimization. The method considers the effect of case hardening by applying a constant volume expansion to an FE model of the tooth, and the resulting residual stresses are superimposed to stress history results. Once the series of stress history steps have been obtained, Findley multiaxial fatigue criteria are used to determine the risk of fatigue crack initiation. This paper reproduces results obtained by MackAldener using the proposed methodology, and good agreement is observed.

INTRODUCTION

Gears are case hardened to produce residual compressive stresses at the surface, which improves wear resistance, bending, and contact fatigue strength. These compressive stresses are balanced by tensile stresses in the core. This poses an increased risk of fatigue crack initiation in the material below the surface. The failure mode where a subsurface fatigue crack initiates close to case-core boundary, approximately mid-height of the tooth, is called Tooth Interior Fatigue Fracture (TIFF) or Tooth Flank Fracture (TFF, sometimes also known as Tooth Flank Breakage or TFB). The location of the crack initiation distinguishes this failure mode from other fatigue failure modes. Previous research [1-8] has established that the directions in which the crack progresses and the appearance of the associated fracture surface are dependent on the flank loading. Although there does not appear to be total agreement in the literature, TIFF (failure with reverse loading) and TFF (failure with single flank loading) appear to have very similar characteristics and crack initiation mechanisms. The final fracture shape is different, due to TIFF having near symmetric total stresses along the tooth centerline (with two possible initiation points per tooth). They can be analyzed using the same approaches.

This type of failure appears at loads below the allowable loading conditions for pitting and bending fatigue failure modes based on standard calculation procedures [9]. Therefore, understanding of such failure is required at the design stage of transmission systems.

Here, a summary is given of the current calculation methods found in the literature for both TIFF and TFF. The currently proposed approaches for TIFF and TFF all have similar fundamental approaches consisting of four stages:

- Calculation of stress history
- Calculation or specification of residual stresses
- Calculation of equivalent stresses using some fatigue criteria
- Comparison with some initiation thresholds

The differences between the methods lie in the details of the above steps. Further, the applicability of the methods depends on the implementation details of these steps and the assumptions made at each stage.

The calculations of each step could be interchanged between methods creating a number of permutations of possibilities. TIFF and TFF has been shown to depend on gear macro geometry, loading, material, and hardening properties. Currently, there is no accepted international standard to assess the probability of TIFF and TFF[1] failures for a given design and therefore no standardized method to assess the relative importance of the influencing factors.

Tooth Interior Fatigue Fracture Calculation Methods
MackAldener [1-3] has shown that an analysis method based on two-dimensional Finite Element Analysis (FEA) can be utilized to analyze the risk of TIFF and

---

[1] The ISO committee is currently working on a draft standard, ISO/DTR 19042, for the calculation of Tooth Flank Fracture performance.

determine the optimum macro geometry, material, and case hardening properties. In this analysis, MackAldener used the gear Loaded Tooth Contact Analysis program LDP (load distribution program) to calculate the total force on one tooth at different phases within the mesh cycle. The calculated force was then applied to the FE mesh as a torque after normalizing with the face width. A contact analysis was then run on the 2D FE model in order to calculate the stress history. MackAldener's early paper [1] assumed constant material properties for case and core. However, because the gear is case hardened, the material fatigue properties will not be the same throughout the tooth. This assumption was removed in later papers where non-homogenous fatigue properties were used in the case region. Fatigue properties were assumed to vary with depth in the same way as the hardness profile. The methodology used in this paper is based on MackAldener's FE-based analysis method and therefore further details of MackAldener's methodology and results are discussed in later sections.

Due to the complexity of setting up and running MackAldener's FE-based method within a general FE package, MackAldener [2] also proposed a simpler semi-analytical method for rapid calculation, design parameter studies, and optimization, but with some compromise in the accuracy of results. In the analysis results presented in MackAldener [2], results differed between this method and MackAldener's FE-based method by a maximum of 20 percent. This method was seen to over-predict the risk of TIFF.

MackAldener concluded that TIFF can be avoided if the slenderness ratio is reduced, tensile residual stresses are reduced, the gear is not used as an idler gear, and optimum case and core properties are used. MackAldener's TIFF methodology can be used to investigate TFF as well as TIFF, simply by considering single flank loading instead of reverse loading. However, crack initiation thresholds could be different and require experimentation or field data to clarify.

Tooth Flank Fracture Load Capacity Calculation Methods
To the author's knowledge, there are two main TFF load capacity calculation methods proposed in the literature.

The first is a calculation method for TFF load capacity proposed by Witzig [8]. This method has been published in Witzig [8], Tobie et al. [6], and Boiadjev et al. [7]. The method relies on calculation of the local stress history based on a shear stress intensity hypothesis of Foppl [10]. The method has significant empirical contributions and is limited in applicability due to the empirical nature of the equation used in the shear stress intensity hypothesis. In the literature, this equation has been presented for single contact point only; it could, in theory, be extended to consider two contact points (i.e., reverse loading) but this is not trivial. The method as published is also restricted to case hardened gears due to the assumptions in the residual stress calculation. It should also be noted that the proposed method in its current form can under-estimate the crack initiation risk if resulting tensile stresses within the core are not small, since these resulting tensile stresses are currently neglected. However, this simplification may only be reliable when the core section is much larger when compared to the thickness of the case. This introduces limitations on applicability for slender teeth and extensive case hardening depths.

Ghribi and Octrue [5] proposed an alternative calculation method for TFF load capacity. This method is more generic than that of Witzig [8] and can be applied to both Tooth Flank Fracture and TIFF. The method proposes use of a multiaxial

fatigue criterion and considers the importance of including tensile stresses in the core. The stress history is calculated using the Hertzian contact calculations of ISO TR 15144-1 [11], together with a proposal of Johnson for the stress at a depth inside the tooth. Method A of ISO TR 15144-1 [11] is based on using the results of a 3D gear Loaded Tooth Contact Analysis, however, only contact stresses calculated by the standard have been considered in these analyses. The addition of stresses due to bending has been mentioned as planned future work.

None of these methods include an FEA-based methodology, although they clearly could be adapted to do so. However, using general FE packages, this requires considerable time and computational power to set up and run analyses.

In the following section, the models used within this paper are outlined. Justification is given for model selection, and the formulation described is used throughout the remainder of this paper. The results section demonstrates the use of the described methodology as a means to investigate the risk of fatigue crack growth beneath the surface. The influence of various parameters has been investigated. Good validation against previously published data is shown for the prediction of Crack Initiation Risk Factor.

METHODOLOGY AND ANALYSIS
The following methodology used for the analysis of TIFF has been implemented in SMT's MASTA Release 7.

MASTA's implementation is derived from MackAldener's finite element method, but the need for a full FE tooth contact analysis has been removed by using loading conditions calculated using MASTA's specialized Loaded Tooth Contact Analysis. MackAldener also simplified his FE analysis in a later stage, not for the calculation of Crack Initiation Risk Factor, but when investigating the crack propagation mechanism during the TIFF [12]. This method removes the complexity of the contact analysis and speeds up the calculation while reducing the computational requirements.

Analysis of the Stress History
MASTA's 3D Loaded Tooth Contact Analysis model combines an FE representation of bending and base rotation stiffness of the gear teeth and blank with a Hertzian contact formalism for the local contact stiffness. This calculation includes the effect of extended tip contact where the effective contact ratio is

increased under load due to tooth bending. This effect can be particularly important for slender tooth gears, which are also more at risk of TIFF.

This model is used to determine load boundary conditions at a selected number of time steps through the mesh cycle. At each time step, the load distribution between and across the teeth is calculated, and at each of the contact lines, the following are obtained:
• Load positions
• Load magnitudes
• Hertzian half widths

A separate fine 2D mesh of the gear tooth is then built automatically using plane strain elements. At each time step within the mesh cycle, the position and the distribution of the load is determined from the results of the 3D tooth contact analysis and applied to the 2D FE mesh using the average load position and Hertzian half width. The force is assumed to lie in the line of action and is normalized by the tooth width (definition used by MackAldener). The contact force was distributed onto the 2D FE model assuming a Hertzian distribution within the Hertzian contact width calculated using the

3D LTCA model. In the following results presented in this paper, the finite element mesh was sized according to the Hertzian half width, and a refinement study was performed to check the convergence of the results.

Residual Stress Analysis

Residual stresses influence the stress states within the gear tooth. These stresses are not load dependent and assumed to be constant over time. Residual stresses due to case hardening and shot peening are superimposed. A separate FEA analysis using the 2D mesh used to calculate the stress history due to flank loading is used to calculate these residual stresses.

The transformation strain profile is isotropic and measured relative to the core. This profile has been presented as a piecewise polynomial with smooth connections by MackAldener [3].

$$\varepsilon_t(z) = \begin{cases} \varepsilon_1 + 4(\varepsilon_2 - \varepsilon_1)\left(\left(\frac{z}{\bar{z}}\right) - \left(\frac{z}{\bar{z}}\right)^2\right) & \text{if } 0 \leq z \leq \frac{\bar{z}}{2} \\ -4\varepsilon_2\left(1 - 6\frac{z}{\bar{z}} + 9\left(\frac{z}{\bar{z}}\right)^2 - 4\left(\frac{z}{\bar{z}}\right)^3\right) & \text{if } \frac{\bar{z}}{2} \leq z \leq \bar{z} \\ 0 & \text{if } \bar{z} \leq z \end{cases}$$

Equation 1

where: ε_1 is the transformation strain at the surface, ε_2 is the maximum transformation strain, z is the normal depth at the point considered, and $\bar{z}$ is the total case depth.

The volume expansion in the surface layer due to the case-hardening process is modeled by applying a temperature profile. The temperature profile applied is the same as the transformation strain profile when the coefficient of thermal expansion is set to 1. All side nodes are allowed to move only in the radial direction.

Figure 1 shows the results presented by MackAldener for the variation of residual stresses with depth beneath the surface both using the analysis method previously described and from measurements carried out by MackAldener. This residual stress profile is a result of the transformation strain profile. Figure 1 further compares this residual stress profile with that proposed by Lang [13] and used by Witzig [8] in the investigation of TFF. Interestingly, the profiles differ quite significantly. This may be due to a significant material dependency not considered, but the reason is not currently known and needs to be understood further.

In this study, the residual stress profile, which is the result of the strain profile, has been utilized with ε_1=0.000833 and ε_2=0.00114 as determined by MackAldener [3]. It should be noted that the resulting calculated residual stresses can change from one mesh position to another due to the variation in tooth thickness.
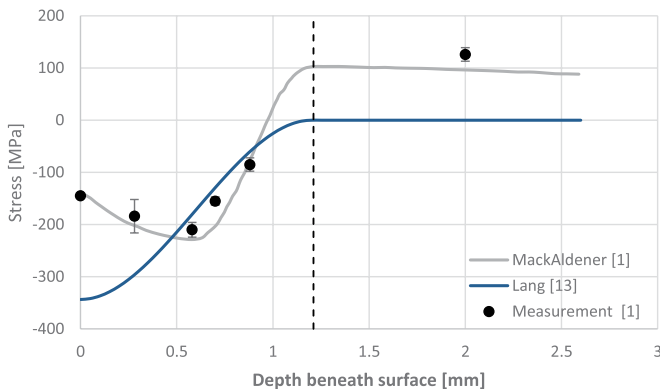

Figure 1: Variation of residual stresses with increasing depth. The total case depth is marked by a dashed line.

Final Stress State and Fatigue Crack Initiation Criterion

The effective stress state within the gear teeth during its load cycle is calculated, without calculating residual stresses at each step, by superimposing the calculated stress history states and the estimated residual stresses.

The Findley multiaxial fatigue criterion [14] is then used to analyze the stress history and assess if failure is going to occur. Within this paper's analysis, the Findley critical plane stress has been calculated for every 5 degrees of inclination at each node. The value of 5 degrees was chosen, instead of every 1 degree used by MackAldener [2], as results did not show a significant dependency on this value. This was confirmed by the cases shown in the results section of this paper where the difference between using an inclination increment of 2.5 degrees is less than 0.05 percent.

The Findley stress is calculated as:

$$\sigma_F = \tau_a + a_{cp}\sigma_{n,max}$$

Equation 2

where τ_a is the shear stress amplitude, $\sigma_{n,max}$ is the maximum normal stress, and a_{cp} is the material fatigue sensitivity to normal stress. Variation of the material properties within the tooth are related to the hardness profile as described in the following section.

The ratio between the maximum Findley critical plane stress and critical shear stress is a measure of the risk of crack initiation. This metric is called the Crack Initiation Risk Factor, or CIRF.

Hardness Profile and Material Properties

The variation of the material properties within the case and core play an important role in TIFF. However, many assumptions have been made in previous analyses in this area. Because the analyzed gear is case hardened, the material properties are not the same throughout the tooth. Hence, the critical shear stress, and the fatigue sensitivity to normal stress, in the critical plane criterion are also expected to vary from place to place. As with MackAldener, for this paper's analysis, we have assumed that these properties vary in the same way as an assumed hardness profile.

$$H(z) = H_{surface}g\left(\frac{z}{\bar{z}}\right) + H_{core}\left(1 - g\left(\frac{z}{\bar{z}}\right)\right)$$

$$g\left(\frac{z}{\bar{z}}\right) = 1 - 3\left(\frac{z}{\bar{z}}\right)^2 + 2\left(\frac{z}{\bar{z}}\right)^3$$

Equation 3

where, $H_{surface}$ is the hardness at the surface, H_{core} is the hardness at the core, g is the function that determines the variation between the case and the core defined by MackAldener, z is the normal depth at the point considered, and $\bar{z}$ is the total case depth.
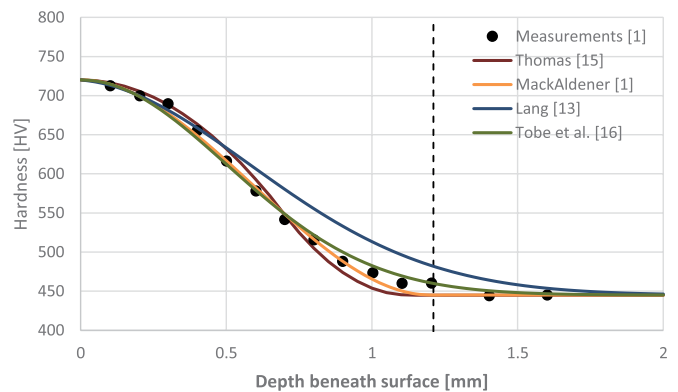

Figure 2: Experimentally measured hardness profile and curve fits of MackAldener together with a number of empirical models available in the literature. The total case depth of 1.2 mm is marked by a dashed line. Effective case depth where hardness drops below 550 HV is 0.68 mm (required for empirical models).

Factor	Description	Low level	Nominal level	High level
A	Critical plane stress within the core	359.85 MPa	479.8 MPa	559.75 MPa
B	Fatigue sensitivity to normal stress within the core	0.28	0.37	0.46
C	Gear design	Slender	Original	Not-Slender
D	Total case depth	0.9 mm	1.2 mm	1.5 mm
E	Torque on the pinion	1238 Nm	1651 Nm	2064 Nm

Table 1: Summary of factors used in the factorial design [2]

	Slender		Original		Not-Slender	
	Pinion	Wheel	Pinion	Wheel	Pinion	Wheel
Module [mm]	2.34		3.06		3.75	
Pressure angle [°]	17.5		20		22.5	
Helix angle [°]	15					
Center distance [mm]	166.5					
Face width [mm]	43	35	43	35	43	35
Tip diameter [mm]	116.5	230.6	116.5	230.6	116.5	230.6
Profile shift coefficient	0.270	-0.669	0.65	0.250	0.6	0.895
Protuberance [mm]	0.06	0.095	0.06	0.06	0.06	0.06
Addendum for tool [mm]	4.85	3.9	4.35	4.35	4.35	4.8
Protuberance angle [°]	5.044	8.342	3.045	3.045	4.308	3.786
Tool edge radius [mm]	0.45	0.85	1.2	1.2	1.75	1.45

Table 2: Gear data for the gear designs considered [2]

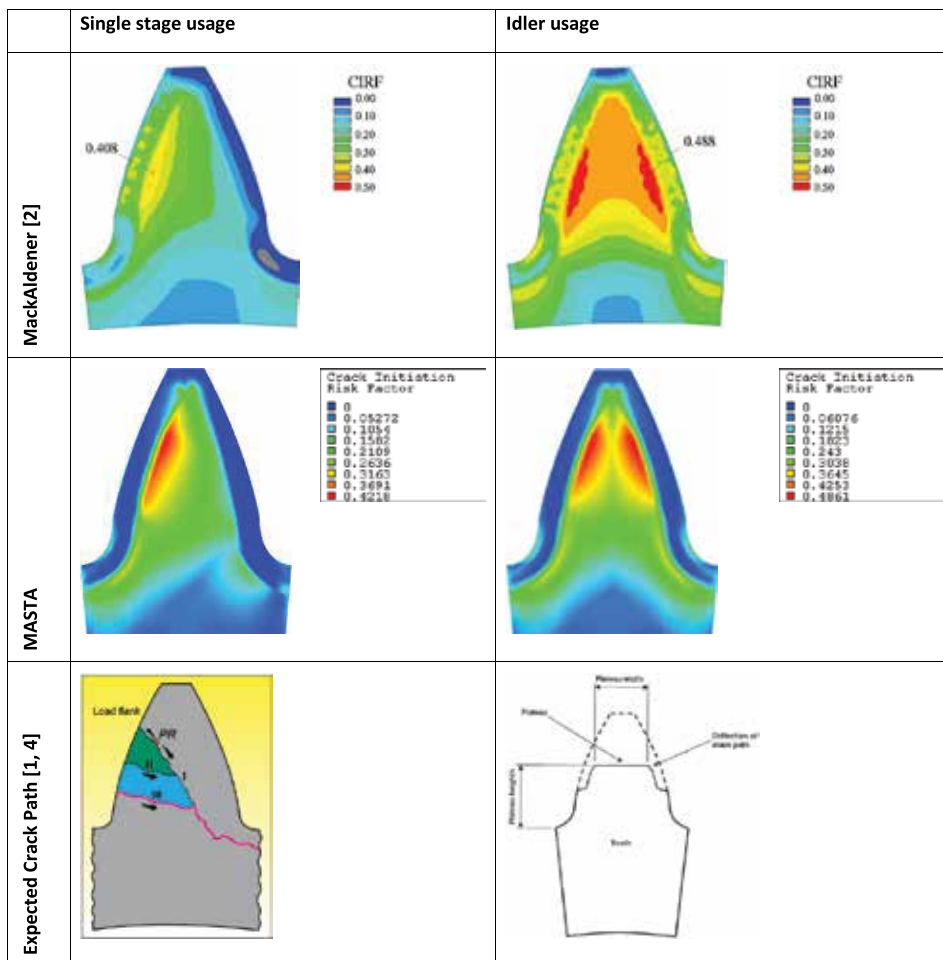|	Single stage usage	Idler usage
MackAldener [2]		
MASTA		
Expected Crack Path [1, 4]		

Figure 3: Comparison of CIRF for single stage and idler loading as calculated by MackAldener and MASTA. Results are presented for the original gear with nominal factors as described in Table 1 and Table 2. Expected crack propagation paths for each loading type are shown.

Figure 2 shows a comparison of the hardness profile measurement and curve fit proposed by MackAldener with other hardness profile models in the literature. For this article, MackAldener's curve fit has been used. It is interesting to note that the hardness profile model proposed by Thomas [15] has been found to give the best comparison against MackAldener's measurement, and that of Tobe et al. [16] is also close. The method of Lang could lead to a difference in the CIRF since fatigue properties are expected to differ near the case/core boundary.

In the current implementation, the material properties are assumed to vary continuously between case and core in the same manner as the hardness profile. This assumption is not required if the variation of the material properties are known.

Critical shear stress, σ_{crit}

$$\sigma_{crit}(z) = \sigma_{crit,\ surface}\, g\left(\frac{z}{\bar{z}}\right) + \sigma_{crit,\ core}\left(1 - g\left(\frac{z}{\bar{z}}\right)\right) \qquad \text{Equation 4}$$

Fatigue sensitivity to normal stress, a_{cp}

$$a_{cp}(z) = a_{cp,\ surface}\, g\left(\frac{z}{\bar{z}}\right) + a_{cp,\ core}\left(1 - g\left(\frac{z}{\bar{z}}\right)\right) \qquad \text{Equation 5}$$

The surface fatigue resistance of a gear flank and root can be improved by shot peening. This improvement is due to an increase in the compressive stresses in a thin layer close to the surface. This layer is very thin compared to the case-hardening layer. Shot-peening properties for depth and the effect on the critical shear stresses are required. In the current implementation, the depth has been assumed constant and the effect on the critical shear stresses assumed to be constant, specified via shot-peening factor.

Assumptions
There are a few points worth noting about the assumptions used within this paper's methodology:
- Two-dimensional analysis has been utilized to analyze risk of TIFF. This option has been considered to be enough by MackAldener [1].
- Material fatigue properties vary in the same way as the hardness profile. These material properties within the case/core boundary has an important role in TIFF.
- The transformation strain profile is isotropic and measured relative to the core. It is also assumed that this profile could be represented by a piecewise polynomial with smooth connections.
- It is assumed that the residual stresses can be superimposed stress history.
- No micro geometry has been included in the FE mesh, but loading conditions include selected micro geometry.
- Friction is not currently included in the LTCA analysis, which provides the load boundary conditions to the TIFF analysis.

VALIDATION RESULTS

This section covers two parts: The first compares contour plots for a single design stage to results obtained by MackAldener; the second

replicates the factorial design experiment run by MackAldener with the results for all 32 designs compared against the reported CIRF values in the literature.

Firstly, contour plots of the calculated CIRF for a single design are compared with MackAldener's results. Figure 3 shows the results for both single stage and idler loading of the gear. For comparison previously proposed [1, 4] crack propagation paths are also shown in Figure 3. In general, the correlation of results is good. It is clear from Figure 1 that MASTA's results are smoother compared to those of MackAldener, as many more time steps have been considered within the mesh cycle in the MASTA solution. Table 1 shows the material factors used within this analysis, with the nominal values used for the results of Figure 3. Other material properties, considered constant throughout the entire study, are critical shear stress, 1090 MPa, and sensitivity to normal stress within the case [1].

Factorial Design

MackAldener conducted a factorial design with five factors. In total, 32 designs have been considered by varying critical plane stress within the core (A), fatigue sensitivity to normal stress within the core (B), gear tooth geometry (C), total case depth (D), and torque on the pinion (E). For each of the factors, two levels, low and high, have been considered; their values are presented in Table 1. Details of the gear tooth geometries are given in Table 2. For each of the designs, the CIRF throughout the tooth was calculated.

Figure 4 shows a comparison of the calculated maximum CIRF for all 32 designs. From Figure 4 it is clear that there is a good overall correlation between CIRF calculated in MASTA and by MackAldener [2]. Some slight deviation in results is seen for designs 13 through 16. These experiments relate to varying torques and varying total case depth for low critical shear stress and high fatigue sensitivity to normal stress within the core for not-slender gear set.

Figure 5 displays the average CIRF results for each value of each factor together with the average for some interactions. It can be seen that good agreement has been observed for factors A, B, D, and E, and reasonable agreement has been observed for factor C. As previously discussed, the lower level of agreement shown for factor C is due to deviations in experiment index 13 to 15. These experiments relate to varying torque and varying total case depth for low critical shear stress and high fatigue sensitivity to normal stress within the core for not-slender gear set. Interaction effects, which include this factor, also are affected by this deviation.

The trends shown in Figure 5 can be used to propose a strategy to avoid a high CIRF. Crack initiation risk can be mitigated by using a material with higher critical shear stress and lower fatigue sensitivity to normal stress within the core, increasing the total case depth and reducing gear tooth slenderness and transmitted torque.

CONCLUSION

An analysis technique based on finite element analysis to analyze risk of TIFF crack initiation has been presented. In this analysis, Loaded Tooth Contact Analysis (LTCA) results obtained from a full 3D elastic tooth contact model have been utilized to determine load boundary conditions.

The key methodologies and conclusions from this paper are the following:

- It is possible to replace a computationally expensive explicitly modeled FE-based contact analysis with simple load boundary conditions obtained by a separate specialized gear Loaded Tooth Contact Analysis, in order to apply MackAldener's methodology for the analysis of TIFF.
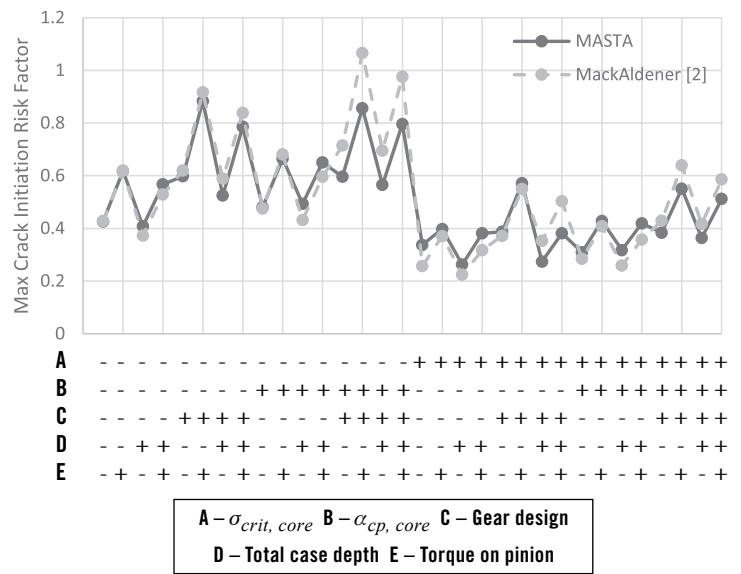

Figure 4: Comparison of the calculated maximum CIRFs from MASTA and MackAldener's finite element calculations.
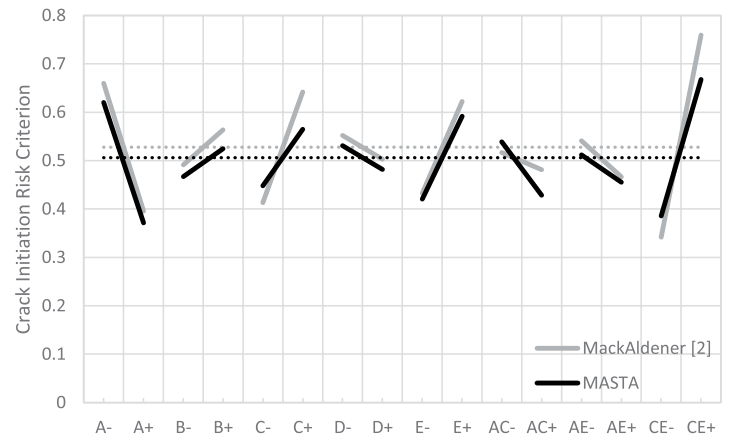

Figure 5: Comparison of main and interaction effects on CIRF response for MASTA and MackAldener's FE calculations. The dotted line represents the mean CIRF response.

- Smoother results have been obtained compared to those of MackAldener's results, due to the number of time steps considered within the mesh cycle.
- A parametric study initially conducted by MackAldener to investigate which parameters influence the risk of TIFF has been repeated to validate the proposed methodology and implementation, and good agreement was achieved.
- MackAldener's findings with regards to possible design options for avoiding TIFF have been confirmed in this study.

Further work on gears loaded on a single flank (i.e., TFF) and comparison of TIFF load carrying capacity with that for other failure modes, such as bending and pitting fatigue, are planned for future work.

REFERENCES

1. MackAldener, M. and Olsson, M. (2000) Interior Fatigue Fracture of Gear Teeth, Fatigue & Fracture of Engineering Materials & Structures, 23 (4), pp. 283-292.
2. MackAldener, M. and Olsson, M. (2000) Design Against Tooth Interior Fatigue Fracture, Gear Technology, Nov/Dec 2000, pp. 18-24.
3. MackAldener, M. and Olsson, M. (2001) Tooth Interior Fatigue Fracture, International Journal of Fatigue, 23, pp. 329-340.

4. Bauer, E. and Bohl, A. (2011) Flank Breakage on Gears for Energy Systems, VDI International Conference on Gears, October 2010. Also Gear Technology. November/December 2011.

5. Ghribi, D. and Octrue, M. (2014) Some theoretical and simulation results on the study of the tooth flank breakage in cylindrical gears, International Gear Conference, Lyon, France, 26-28 August 2014.

6. Tobie, T.; Höhn, B. R. and Stahl, K. (2013) Tooth Flank Breakage – Influences on Subsurface Initiated Fatigue Failures of Case Hardened Gears. Proceedings of the ASME 2013 Power Transmission and Gearing Conference, Portland, OR, 4th-7th August 2014.

7. Boiadjiev, I.; Witzig, J.; Tobie, T. and Stahl, K. (2014) Tooth flank fracture – basic principles and calculation model for a sub-surface initiated fatigue mode of case hardened gears, International Gear Conference, Lyon, France 26-28 August 2014. Also Gear Technology. August 2015.

8. Witzig, J. (2012) Flankenbruch Eine Grenze der Zahnradtragfähigkeit in der Werkstofftiefe. PhD Thesis, Technical University of Munich.

9. BS ISO 6336-1: 2006 Calculation of load capacity of spur and helical gears – Part 1: Basic Principles, Introduction and General Influence Factors.

10. Föppl, L. (1947) Drang und Zwang, Band III – Eine höhere Festigkeitslehre für Ingenieure. Leibniz Verlag, München.

11. BS ISO/TR 15144-1:2014 Calculation of micropitting load capacity of cylindrical spur and helical gears – Part 1: Introduction and basic principles.

12. MackAldener, M. and Olsson, M. (2002) Analysis of Crack Propagation during Tooth Interior Fatigue Fracture, Engineering Fracture Mechanics, 69, pp. 2147-2162.

13. Lang, O. R. (1979) The dimensioning of complex steel members in the range of endurance strength and fatigue life, Zeitschrift fuer Werkstofftechnik, Vol. 10, p. 24-29.

14. Findley, W. N. (1959) A Theory for the Effect of Mean Stress on fatigue of metals under combined torsion and axial load or Bending. Journal of Engineering for Industry, pp. 301-306.

15. Thomas, J. (1997) Flankentragfähigkeit und Laufverhalten von hartfeinbearbeiteten Kegelrädern. Ph.D. Thesis, Technical University of Munich, Germany.

16. Tobe, T.; Kato, M.; Inoe, K.; Takatsu, N. and Morita, I. (1986) Bending strength of carburized C42OH spur gear teeth. JSME, p. 273-280.

This paper was presented at the British Gear Association (BGA) Gears 2015 Technical Awareness Seminar in November 2015 at Nottingham University.

ABOUT THE AUTHORS: Baydu Al has been an analyst/software engineer at Smart Manufacturing Technology Ltd. (SMT) since October 2014. He has worked as a researcher at Nottingham University in gas turbine and transmission systems and specialized in efficiency and oil management prior to SMT. Since joining SMT, he has been contributing to MASTA's Loaded Tooth Contact Analysis and analysis of Tooth Interior Fatigue Fracture.

Dr. Paul Langlois is the CAE products development department manager at Smart Manufacturing Technology Ltd. (SMT). Having worked for SMT for 10 years, he has extensive knowledge of transmission analysis methods and their software implementation. He manages the development of SMT's software products and was a main contributor to many aspects of the technical software development. He contributes to ISO standards development for gears as a member of the BSI MCE/005 committee.